International Journal of
Molecular Sciences

MDPI

Article

Nerve Growth Factor Peptides Bind Copper(II) with High Affinity: A Thermodynamic Approach to Unveil Overlooked Neurotrophin Roles

Antonio Magrì [1], Diego La Mendola [2,*] and Enrico Rizzarelli [1,3]

[1] Institute of Crystallography, CNR, Via Gaifami 18, 95126 Catania, Italy; leotony@unict.it (A.M.); erizzarelli@unict.it (E.R.)
[2] Department of Pharmacy, University of Pisa, Via Bonanno Pisano 6, 56126 Pisa, Italy
[3] Department of Chemical Sciences, University of Catania, Viale A. Doria 6, 95125 Catania, Italy
* Correspondence: lamendola@farm.unipi.it; Tel.: +39-050-2219533

Abstract: Nerve growth factor (NGF) is a protein essential to neurons survival, which interacts with its receptor as a non-covalent dimer. Peptides belonging to NGF N-terminal domain are able to mimic the activity of the whole protein. Such activity is affected by the presence of copper ions. The metal is released in the synaptic cleft where proteins, not yet identified, may bind and transfer to human copper transporter 1 (hCtr1), for copper uptake in neurons. The measurements of the stability constants of copper complexes formed by amyloid beta and hCtr1 peptide fragments suggest that beta-amyloid (Aβ) can perform this task. In this work, the stability constant values of copper complex species formed with the dimeric form of N-terminal domain, sequence 1–15 of the protein, were determined by means of potentiometric measurements. At physiological pH, NGF peptides bind one equivalent of copper ion with higher affinity of Aβ and lower than hCtr1 peptide fragments. Therefore, in the synaptic cleft, NGF may act as a potential copper chelating molecule, ionophore or chaperone for hCtr1 for metal uptake. Copper dyshomeostasis and mild acidic environment may modify the balance between metal, NGF, and Aβ, with consequences on the metal cellular uptake and therefore be among causes of the Alzheimer's disease onset.

Keywords: copper; NGF; Ctr-1; Alzheimer's; protein; peptidomimetic; potentiometry; stability constants; beta amyloid; metallostasis

Citation: Magrì, A.; La Mendola, D.; Rizzarelli, E. Nerve Growth Factor Peptides Bind Copper(II) with High Affinity: A Thermodynamic Approach to Unveil Overlooked Neurotrophin Roles. *Int. J. Mol. Sci.* **2021**, *22*, 5085. https://doi.org/10.3390/ijms22105085

Academic Editor: Antonello Merlino

Received: 21 April 2021
Accepted: 7 May 2021
Published: 11 May 2021

1. Introduction

Copper performs several essential functions as a cofactor in many enzymes in the living systems and it is required for the development and function of the human brain [1–3]. In recent years, it has been shown that copper, analogously to zinc, plays a role as modulator of cellular signal transduction pathways [4–6]. Copper is stored in synaptic vesicles and is released by electrical depolarization in the synaptic cleft of glutamatergic synapses at concentration values that can reach 100 μM [7]. Copper may have inhibitory or stimulating effect on synaptic plasticity, affecting memory and learning processes although the mechanisms by which the metal performs these functions remain largely undefined [8,9]. The dual effect may be related to the metal binding by different proteins expressed in neurons and released in the synapses as beta-amyloid (Aβ) [10].

The actual biological function of Aβ is still unknown. The polypeptide may control copper efflux in the synapses and it has been demonstrated that the polypeptide improves memory formation [11], synaptic plasticity, and neuronal survival [12].

In particular, the monomeric form of Aβ activates the cyclic AMP response element-binding protein (CREB), which in turn promotes the transcription and release of the brain-derived neurotrophic factor (BDNF) a neurotrophin (NT) strongly involved in long term potentiation (LTP) and memory formation [13].

It is worth noting that it has been demonstrated that copper ions may modulate kinase signaling networks of neuronal tissues induced by neurotrophins [14]. The nerve growth factor (NGF) is the first discovered member of NTs family [15]. NGF is essential for the development, survival, and activity of neurons [16,17]. NGF initiates the signaling pathways through the binding to tropomyosin receptor kinase A (TrkA) triggering a signaling cascade up to the activation of CREB [18,19].

Copper ions enhance NGF functionality and the effect seems related to the presence of metal binding site in the N-terminus domain of NGF [20]. NGF(1-14), a peptide encompassing the first 14 residue of NGF, is able to bind copper ions and mimic whole protein signal transduction activating CREB [21]. The NGF interacts with TrkA as a non-covalent dimer, so a dimeric form of the peptide NGF(1–14) has been tested, showing higher activity than monomers in the release of BDNF [14].

NGF signaling pathways control also the post-translational modifications of the amyloid precursor protein (APP) and then Aβ production in neurons [22–24]. Moreover, the deprivation in NGF determines Aβ aggregation and tau hyperphosphorylation in Alzheimer's disease (AD) [25] while NGF addition protects against cell death and toxicity triggered by Aβ but the underlying mechanism remains unclear [26]. On the other hand, astrocytes activated by Aβ stimulate NGF secretion, whose excess in turn causes the death of hippocampal neurons [27].

In the dynamic environment present at the synaptic cleft, a potential interconnection among copper, Aβ, and NGF, could be one of the key components of the memory formation process.

Therefore, the dyshomeostasis of copper could be at the basis of Aβ and/or NGF dysfunctions; conversely, a malfunction in the metabolic pathways could negatively affect the normal influx of copper into neurons [28]. The consequences could lead to the development of the progressive neurodegenerative disorder such as Alzheimer's disease (AD) [29,30].

In the brains of patients affected by AD, a high copper concentration, up to 0.4 mM, is localized in senile plaques composed of amyloid aggregates [31]; however, the involvement of copper in AD is still controversial [32]. Studies show copper deficiency in patients affected by AD, and consequently a need to enhance copper levels so to restore normal metal concentration [33,34]; differently, other experiments point to metal overload and consequent demand to reduce copper concentration [35,36].

Copper dyshomeostasis with an increase in the labile pool of metal and a parallel decrease in the copper bound to proteins or peptides is the main interpretation [37–39]. A local imbalance of copper between extra- and intra-cellular spaces may drive its binding to Aβ, which may result in formation of oligomeric fibrils, amyloid, or amorphous aggregates, depending on the metal ion/peptide molar ratio.

Aβ may play the role of handling copper cellular influx/efflux via binding metal and transfer it to human copper transporter 1 (hCtr1), the main protein responsible for Cu import into cells [40]. Studies carried out with the peptide model showed that a peptide encompassing the first 14 residues of hCtr1 binds copper ions with higher affinity than N-terminal Aβ peptides [41]. For this reason, it is relevant to know the affinity of Aβ towards copper ions and many studies have been carried out with different techniques to determine the coordination environment of copper complexes formed with Aβ [42,43].

The pH value is another environmental condition that influences Aβ aggregation and Aβ copper binding. The brain pH is imbalanced towards mild acidic condition in aging and patients with AD [44]. A lowering of pH favors Aβ aggregation and strongly alters the release of pro-inflammatory cytokine affecting the uptake of Aβ by microglial cells [45].

Pathologies, such as ischemic stroke, induce a local decrease of extracellular pH due to an inflammatory insult that is as supposed to be an early event in AD progression [46]. Furthermore, the pH influences copper complex speciation with Aβ and mild acidosis can promote conformational changes or reactive oxygen species production promoting Aβ aggregate precipitation [47].

NGF has been postulated as potential therapeutic agent for the treatment of AD and its side effects, as loss of memory, and taking into account that NGF can bind copper ions in the same spaces shared by Aβ, it may be of interest to determine its affinity for copper(II).

Potentiometry is a technique that determines the stability constant values with a certain accuracy and permits also detection of minor species. This experimental technique may be the ideal choice when conditions allow for its application that can be limited by some factors such as poor solubility of longer or hydrophobic peptides. For this reason, potentiometric measurements have been carried out on shorter and more soluble Aβ fragments, in particular the N-terminal ones where the copper binding sites are found [43].

In this paper, we report the stability constant values and copper coordination environment of a 30-mer peptide of NGF, namely the dimeric form of N-terminal domain 1-15 of the protein obtained by disulfide bridge between cysteine units in position 15 (Figure 1). The obtained data are compared to those reported for the monomeric peptide NGF(1-14) encompassing the N-terminal 14 residues of the NGF protein; the comparison of the affinity constants was extended to those obtained in this work on peptide encompassing the reverse rNGF(14-1) and another with a scrambled sNGF(1-14) sequence to highlight the role of primary sequence in copper binding. Finally, a comparison was made between the affinity constants obtained so far with those of the complexes formed by the copper(II) with Aβ and hCtr1 peptides. This comparison can be helpful to elucidate a molecular-level network among Aβ, NGF, and copper uptake by neurons which can alter synaptic activities under pathophysiologically relevant conditions.

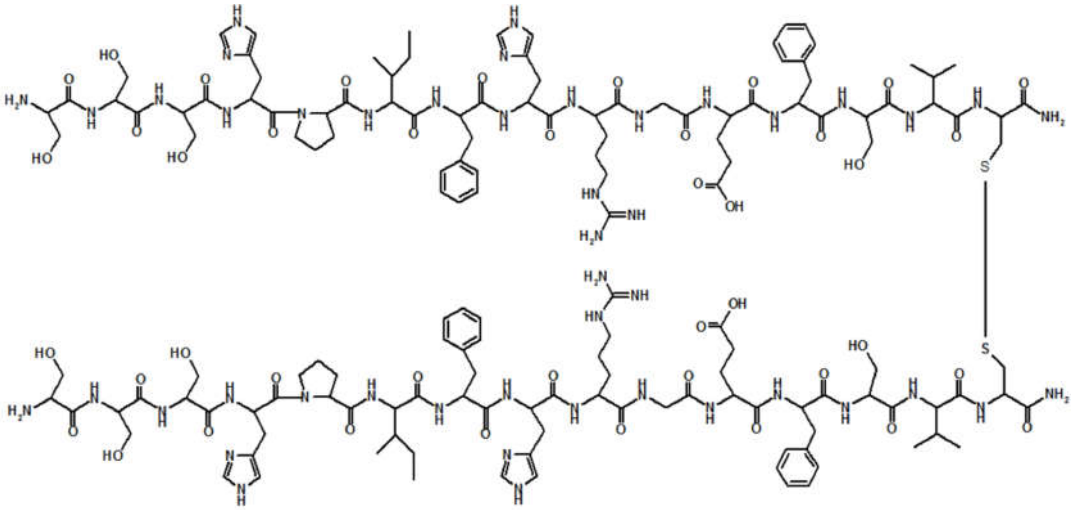

dNGF(1-15)

dNGF(1-15): $(SSSHPIFHRGEFSVC)_2$-NH_2
NGF(1-14) : SSSHPIFHRGEFSV-NH_2
rNGF(14-1) : VSFEGRHFIPHSSS-NH_2
sNGF(1-14) : GFRESPHVSISSH-NH_2

Figure 1. Structure of dNGF(1-15) and primary sequence of NGF N-terminal peptides. In red histidine residues that can act as metal anchoring sites.

2. Results

2.1. Protonation Constants

Peptides protonation constant values were determined by means of potentiometric titrations and are reported in Table 1 together with those of NGF(1-14) peptide. The monomeric ligands rNGF(14-1) and sNGF(1-14) show four proton accepting centers, as ex-

pected. The highest pK value corresponds to the N-terminal amino group. The protonation equilibria of the two histidine residues overlap and the average value for the protonation constant values of the imidazole residues is similar to that reported for analogous peptides [48,49]. The lowest pK value belongs to carboxylate side chain of glutamate and it agrees with that found for other peptides containing glutamic acid residues [50].

Table 1. Protonation constant (log βpqr) and pK values (T = 298 °K and I = 0.1 M KNO_3) [a].

Species	NGF(1-14) [b]	rNGF(14-1)	sNGF(1-14)	dNGF(1-15)
LH	7.56	7.82 (2)	7.85 (3)	7.65 (5)
LH_2	14.13	14.51 (2)	14.65 (3)	15.35 (2)
LH_3	20.14	20.60 (2)	20.87 (3)	-
LH_4	24.44	24.88 (2)	25.11 (4)	28.77 (6)
LH_5	-			35.12 (4)
LH_6	-			41.31 (4)
LH_7	-			46.62 (4)
LH_8	-			50.75 (4)
pK COO^-	4.13	4.28	4.23	4.13
pK COO^-	-	-	-	5.28
pK His	6.01	6.09	6.22	6.21
pK His	6.57	6.69	6.81	6.35
pK His (×2)	-	-	-	(6.71 × 2)
pK NH_2	7.56	7.82	7.85	7.65
pK NH_2	-			7.70

[a] Standard deviations (3σ values) are given in parentheses. [b] Reference [20].

The dimeric peptide d(NGF1-15) was obtained by disulfide bridge between two units of the sequence 1–15 of the protein, exploiting the cysteine present in position 15. Therefore, the number of protonation sites is double compared to that of monomeric peptides, scrambled and reverse. The pK values of N-terminal groups are very similar to that of monomer NGF(1-14). Protonation reactions of the four imidazole side chains take place in completely overlapping reactions and the measured pK values are in a range between 6.7 and 6.2. The pK value of one carboxylate is the same of monomer peptide NGF(1-14) whereas the other carboxylate is significantly less acidic with a pK of 5.28.

2.2. Speciation and Characterization of Copper-Peptide Complexes

The stability constants of the Cu^{2+} complexes are listed in Table 2. The metal ion speciation for each peptide, at 1:1 metal-to-ligand molar ratio, is shown in Figure 2.

[CuLH] is the first complex species formed by rNGF(14-1) and sNGF(1-14) and reaches its maximum percentage of formation at pH 5 (Figure 2). The calculated stability constant values ($\log K_{(111)} = \log\beta_{(111)} - \log\beta_{(011)}$) are 6.33 and 6.12, for rNGF(14-1) and sNGF(1-14) respectively; the value obtained for reverse sequence is more similar to that of NGF(1-14) ($\log K_{(111)}$ = 6.53). The logK(111) values are in the range 6.0–6.5, then higher than those of similar Cu^{2+} complexes of peptide fragments in which the metal ion is bound to one imidazole nitrogen and one carboxylate [48,51,52]. Indeed, these values are in good agreement with those reported for analogous complex species formed by Aβ peptide fragments for which metal ions have been shown to form a macrochelate with a $2N_{im}$, COO coordination mode (log K = 6.18) [53,54].

Table 2. Stability constants (log βpqr) and pK values of copper(II) complexes [a].

Species (pqr) [b]	$\log\beta_{pqr}$ NGF(1-14)[c]	$\log\beta_{pqr}$ rNGF(14-1)	$\log\beta_{pqr}$ sNGF(1-14)	$\log\beta_{pqr}$ dNGF(1-15)
$CuLH_5$	-	-	-	41.18 (3)
$CuLH_3$	-	-	-	31.56 (2)
$CuLH_2$	-	-	-	25.91 (5)
CuLH	14.09	14.15 (1)	13.97 (4)	17.79 (5)
CuL	8.72	8.77 (1)	8.32 (5)	8.21 (4)
$CuLH_{-1}$	3.27	2.33 (2)	−2.74 (3)	-
$CuLH_{-2}$	−4.02	−6.15 (4)	−5.58 (8)	-
$CuLH_{-3}$	−13.34	−14.67 (2)	−13.27 (4)	-
pK (n/m)				
pK (5/3)	-	-	-	4.81 × 2
pK (3/2)	-	-	-	5.65
pK (2/1)	-	-	-	8.12
pK (1/0)	5.37	5.38	5.65	9.57
pK (0/−1)	5.45	6.43	5.57	-
pK (−1/−2)	7.29	8.48	8.33	-
pK (−2/−3)	9.30	8.52	7.69	-

[a] Standard deviations (3σ values) are given in parentheses; [b] pCu + qH + rL = $Cu_pH_qL_r$; $\beta_{bqr} = [Cu_pH_qL_r]/[Cu]_p[H]_q[L]_r$; [c] Ref. [20]. Charges are omitted for clarity; pK(n/m) values reflect the pK value of copper(II) complexes; [L] = 1×10^{-3} M; molar ratio 1:1.

Table 3. Spectroscopic parameters of Copper (II) complexes.

Peptide	pH	UV-vis λ (nm) (ε (M^{-1} cm^{-1}))	CD λ (nm) (Δε (M^{-1} cm^{-1})
rNGF(14-1)	5	640 (64)	280 (−0.30); 316 (+0.20); 670 (−0.27)
	6	625 (144)	280 (−0.40); 323 (+0.33); 671 (−0.44)
	7.4	609 (178)	280 (−0.30); 314 (−0.22); 352 (+0.07); 508 (+0.31); 625 (−0.60)
	9	532 (194)	280 (−1.30); 484 (+0.46); 589 (−0.79)
	10	522 (232)	280 (−1.80); 483 (+0.54); 577 (−1.00)
sNGF(1-14)	5	670 (40)	289 (−0.20); 328 (+0.12); 647 (−0.04)
	6	617 (94)	287 (−1.34); 328 (+0.68); 617 (−0.59)
	7.4	603 (102)	288 (−1.38); 329 (+0.82); 603 (−0.72)
	9-10	522 (141)	306 (+1.47); 544 (−1.13)
dNGF(1-15)	5	635 (50)	280 (−0.34); 321 (+0.19); 669 (−0.24)
	6	612 (70)	280 (−0.40); 323 (+0.33); 671 (−0.44)
	7.4	569 (94)	280 (−1.80); 324 (+0.92); 504 (+0.08); 611 (−0.30)
	8	561 (104)	280 (−2.04); 323 (+0.98); 496 (+0.11); 586 (−0.34)
	9	554 (119)	280 (−2.15); 324 (+0.98); 496 (+0.08); 587 (−0.38)
	10	530 (138)	280 (−2.14); 324 (+0.71); 563 (−0.46)

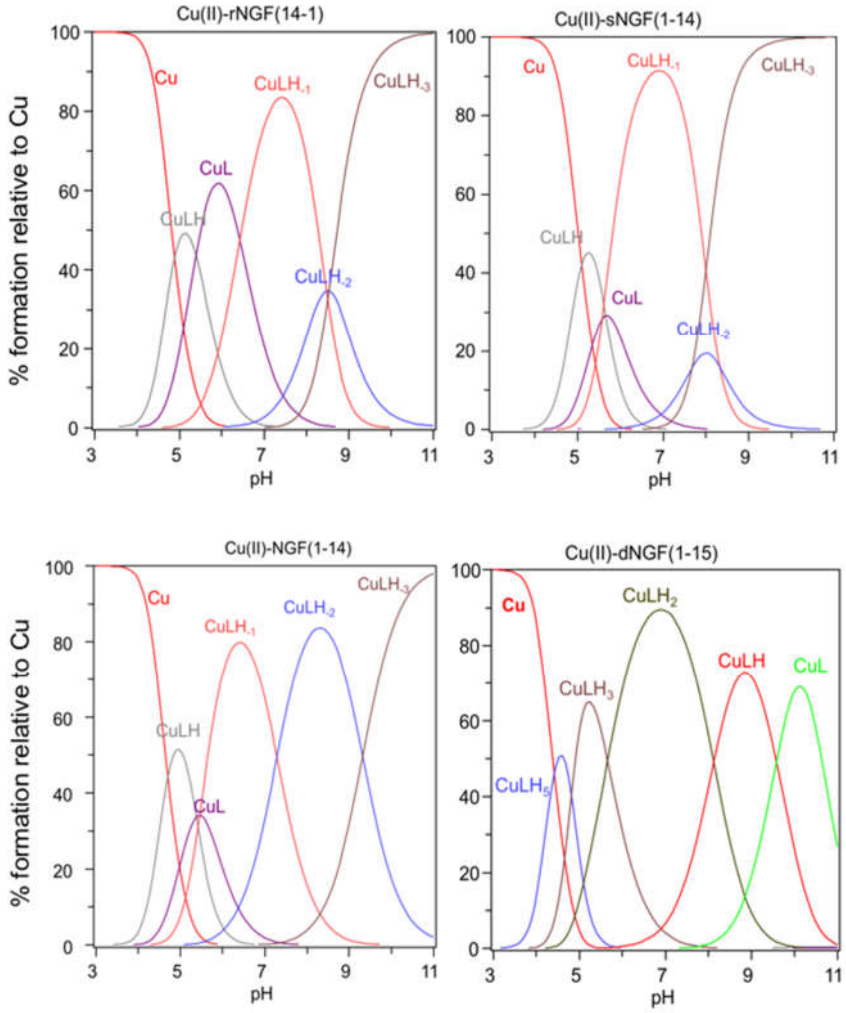

Figure 2. Species distribution of copper(II) complexes with rNGF(14-1), sNGF(1-14), NGF(1-14) and dNGF(1-15). [L] = 1×10^{-3} M; metal to ligand molar ratio of 1:1.

Spectroscopic parameters measured at pH = 5, confirm the $2N_{Im}$,COO^- coordination mode for copper ion and the higher stability of metal complex formed by reverse (λ_{max} = 640 nm, ε = 64 M^{-1} cm^{-1}) compared to scrambled peptide (λ_{max} = 670 nm, ε = 40 M^{-1} cm^{-1}) (Table 3). However, it must be underlined that the parameters are partly influenced by the presence of other species other than free copper.

Increasing the pH, [CuL] complex species is formed. This species is a minor one but the obtained logβ value suggest the involvement of a further donor atom as N-terminal group for both peptides. The reverse peptide also shows for this species a higher value than scrambled one and very similar to that reported for NGF(1-14).

The contemporary presence of an isomer in which a deprotonated amide is bound to metal instead of an amino group, that remains still protonated, cannot be ruled out.

In particular the Cu-rNGF(14-1) system shows a CD signal centered around 320 nm, that is diagnostic of a charge transfer from a deprotonated amide nitrogen to copper ion [55] (Figure 3).

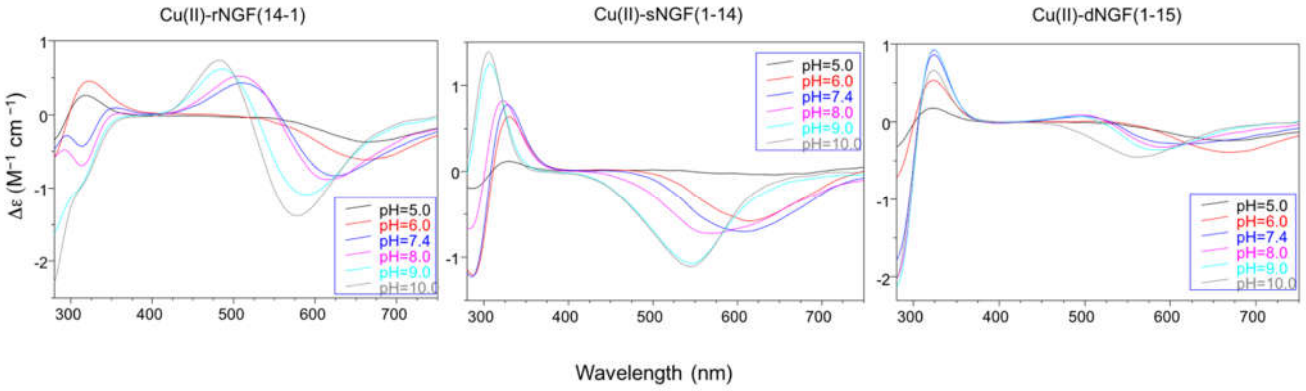

Figure 3. Circular Dichroism spectra with: rNGF(14-1), sNGF(1-14), and dNGF(1-15). [L] = 1×10^{-3} M; metal to ligand molar ratio of 1:1.

The next species formed, [$CuLH_{-1}$], is the predominant complex in the pH range 6.5–8.0. The stepwise constant values $logK_{(11-1)}$ ($logK_{(11-1)} = log\beta_{(110)} - log\beta_{(11-1)}$) are 6.43 for rNGF(14-1) and 5.57 for sNGF(1-14). Both values indicate the deprotonation of an amide nitrogen atom but this step is more favored for sNGF(1-14). The UV–vis parameters are similar suggesting an analogous coordination environment of metal ion with three nitrogen atoms involved in the binding. CD spectra show the diagnostic signal of deprotonated amide nitrogen bound to copper ion even though the conformational features of two peptides are different due to distinctive primary sequence (Figure 3).

As the pH increases, the second deprotonation occurs but it is less favored than the third nitrogen amide deprotonation step. Indeed, the [$CuLH_{-2}$] complex species is a minor one for both peptides, suggesting that the coordination of successive amide nitrogen deprotonation reactions are accompanied by the rearrangement of the peptide metal binding sites [56]. Namely, the histidine imidazole moiety and the subsequent amide are the primary binding sites below pH 8.5, but they are partly replaced by the amino group and preceding amide functions at higher pH values. This effect is supported by significant blue shift of the absorption spectra as well as of the CD band characteristic of peptide amino-bonded copper(II) complexes [57].

The first species formed by dimeric peptide dNGF(1-15) is [$CuLH_5$] that reaches its maximum percentage at pH 4.5 (Figure 2).

The stability constant ($logK_{(115)} = log\beta_{(115)} - log\beta_{(015)} = 41.18 - 35.12 = 6.06$) is indicative of a 2Nim, COO^- coordination mode analogous to monomeric peptides and Aβ as above reported. This is further confirmed by UV–vis parameters similar to that of rNGF(14-1) copper complex. It is to note that in the [$CuLH_5$] species there are only three deprotonated centers and therefore the involvement of $2N_{im}$ requires that one carboxylate group is still protonated. The unusual high pK value of one carboxylate moiety (pK = 5.28) and the pH range of species existence, between 4.0–5.5, makes this hypothesis plausible.

[$CuLH_3$] is the next species formed with a maximum percentage of formation around pH 5.5 (Figure 2). It is not possible to calculate the stepwise stability constant value as performed for other species because the protonation constant of the [LH_3] species was not experimentally obtained. However, the difference with the stability constant of [$CuLH_5$] ($logK_{(112)} = log\beta_{(115)} - log\beta_{(113)} = 9.62$) suggests the deprotonation of the carboxylate not coordinated to copper ion and the binding of another nitrogen atom (imidazole or amino) to the metal ion.

[$CuLH_2$] is the predominant species at physiological pH; the stability constant value logK ($logK_{(112)} = log\beta_{(112)} - log\beta_{(012)} = 10.56$) is high and can be related with the relevant blue shift in the UV–vis maximum absorption (λ_{max} = 569 nm, ε = 94 M^{-1} cm^{-1}). All these data are indicative of a strong ligand field around copper ion, determined by four nitrogen atoms coordination mode in a planar arrangement. It can be assumed that the (NH_2, N^-) five-

membered chelate is assisted by the macrochelation with the N_{Im} donor of the His-4 residue of the same chain and the other histidine belonging to the other chain of dimeric peptide.

The CD spectra show an increase in the wide band centered at 324 nm, that include charge transfer signals of both imidazole and deprotonated amide to metal ion, and a d–d transition band with a relatively low intensity compared to the analogous species formed by monomeric peptides. These CD features are in agreement with the involvement of more imidazole side chain in the metal binding (Figure 3).

The next species [CuLH] and [CuL] show similar spectroscopic parameters to those of [$CuLH_2$], suggesting the deprotonation of amino/imidazole not bound to metal ion and afterwards, at strongly basic pH, the deprotonation of an amide nitrogen atom that substitutes one imidazole in the coordination to metal ion.

3. Discussion

The peptide NGF(1-14) encompasses the first fourteen residues of the N-terminal domain of NGF protein. In a previous paper, we have demonstrated that NGF(1-14) and its dimeric derivative dNGF(1-15) form strong and significant interactions with TrkA, the specific NGF receptor, but not its reverse rNGF(14-1) nor the scrambled s-NGF(1-14) sequence [14]. However, in the presence of copper ions, both peptides NGF(1-14) and dNGF(1-15), induced signaling pathways independently by the receptor activation [14,21]. Conversely, the addition of copper has no effect on neuron cell models treated with rNGF(14-1) or sNGF(1-14) [14]. In a receptor-independent signaling processes, a different copper coordination environment may explain the absence of activity of scrambled and reverse sequence peptides compared to NGF(1-14) and dNGF(1-15).

Therefore, the peptides rNGF(14-1) and sNGF(1-14), designed to highlight the specificity of the primary sequence in the receptor recognition, can also unveil the critical role of the histidine residues with respect to the N-terminal amino group in the metal complex formation.

The protonation constants of two peptides rNGF(14-1) and sNGF(1-14) are similar to each other and to the values reported for the NGF(1-14). This indicates the absence of electrostatic bonds between the side chain groups.

In a peptide, the pK range of protonation centers of the same type, for instance imidazole, widens as their number increases. A peptide encompassing three or more histidine residues shows a pK range of imidazole nitrogen atoms between 5.0–7.5 [58–61]. In the case of the dimeric peptide dNGF(1-15), the pK values determined for the amino and imidazole groups are very similar to those reported for the monomer peptides, indicating the absence of specific interactions between groups belonging to different peptidic chains. A different effect is observed only for the carboxylic groups: the monomer NGF(1-14) and the dimer dNGF(1-15) display a similar pK value for one carboxylate whereas a higher pK value is observed for the second carboxylate group of the dimer dNGF(1-15), indicating a marked reduction of acidity. This suggests a strong electrostatic interaction between the carboxylic anion of the first carboxylic group and the still protonated of the second one.

At acidic pH, there is a certain similarity in the copper complex formation between the investigated peptides whereas at physiological pH, the metal displays a different coordination environment when bound to wild type NGF(1-14) and dNGF(1-15) in comparison with the reverse and scrambled sequences.

In the complex species [CuLH] the copper ion displays a $2N_{Im}$,COO^- coordination mode for both rNGF(14-1) and sNGF(1-14). The reverse sequence peptide shows a higher copper complex stability constant of the macrochelate than sNGF(1-14); an effect due to the closer proximity of the two histidine residues and to the presence of a proline in between, that favors peptide bending and then the macrochelate formation (HFIPH vs. HVSISSH, for rNGF(14-1) and sNGF(1-14) respectively, see Figure 1).

Taking into account the higher number of protonation sites, [$CuLH_5$] is the species formed by dNGF(1-15) analogous to [CuLH] detected for monomeric peptides. [$CuLH_5$] is the first species formed by dNGF(1-15) and starts at a slightly lower pH compared to monomeric peptides, due to differences in protonation constant values. The spectroscopic

parameters are similar to those reported for rNGF(14-1) and the stability constant is in agreement with a $2N_{Im}$,COO^- coordination mode but it is not possible to define if histidine residues involved in metal binding belong to the same chain or not.

At physiological pH, the [$CuLH_{-1}$] is the predominant species for both rNGF(14-1) and sNGF(1-14). The deprotonation step involve an amide nitrogen for both peptides but with a higher value for rNGF(14-1) compared to sNGF(1-14), 6.43 and 5.57, respectively. This difference suggests that the deprotonation does not occur at the amino terminus as in this case a similar value would be expected for the two peptides. Therefore, the deprotonation involves an amide of a histidine residue and the difference between rNGF(14-19 and sNGF(1-14) may be ascribed to proline amid the two histidine for reverse fragment (HFIPH). Indeed, the proline residue acts as a 'break-point' in copper ion coordination [62]. This results in a greater distortion of metal coordination plane for rNGF(14-1) as indicated by the high molar absorption coefficient value of UV–vis maximum absorption. Therefore, at physiological pH, copper bound to both scramble and reverse shows a different speciation and coordination environment compared to NGF(1-14) where the N-terminal amino group is involved in the metal binding [20]. In the wild type sequence, histidine is the fourth residue (His-4), then closer to the terminal amino group. Therefore, the sequence SSSH (see Figure 1) favors the simultaneous involvement of the amino and imidazole nitrogen atoms, prompting a greater stability of the copper complexes.

At physiological pH, [$CuLH_2$] is the predominant species formed by dNGF(1-15). In this species the copper coordination is different from that observed for scrambled and reverse peptides. The stability constant value is higher and indicative of a strong ligand field around copper ion, confirmed by the difference in the UV–vis maximum absorption (λ_{max} = 569 nm) clearly more shifted towards blue compared to the species formed by rNGF(14-1) and sNGF(1-14). The difference observed is due to the involvement of the amino group in metal coordination so to determine a four nitrogen atoms (NH_2, N^-, $2N_{im}$) coordination mode in a planar arrangement. The amide deprotonation is more favored at Ser-2 due to five-membered chelate ring formation than at His-4 where the deprotonation process could form a six-membered chelate ring [63]. The stability constant of copper complex species formed by dNGF(1-15) is higher than that reported for monomer NGF(1-4). The presence of more histidine residues allows to involve the imidazole unit that determines a stronger coordination without inducing relevant distortions in peptide conformation.

This type of coordination is also confirmed by the ease with which successive species are formed, increasing pH. Indeed, the next deprotonation steps involve the side chains not directly involved in the metal binding, and, at a more basic pH, the amide nitrogen of Ser-3; this is further confirmed by the CD spectra that display the same conformational features even at increasing pH values.

It is to note that dimeric peptide does not form species with two copper atoms, confirming that amide deprotonation occurs in one of the two peptidic chains while the other one contributes with the coordination of one or two side chain imidazole groups to the overall stability of the copper complexes.

The determination of the copper complexes stability constants formed by peptides of biological interest is a parameter that provides the affinity of a metal ion for a ligand on a quantitative basis. This can give insights for understanding the activity of such systems, while bearing in mind that the biological matrix is more complex and not an easy task [64].

However, the direct comparison between the stability constant values cannot provide the indication on which peptide binds metal ions more strongly since, as discussed above, they can form complex species with different deprotonation state [65]. For this reason, the apparent dissociation constant, K_D^{app}, is often used to describe, in the biological field, the affinity of a metal to a protein or a peptide. The K_D^{app} is associated with equilibrium

$$ML \leftrightarrow \mathrm{M} + \mathrm{L} \quad (1)$$

and it is given by

$$K_D^{app} = \frac{[M]\,[L]}{[ML]} \quad (2)$$

Therefore, the K_D^{app} provides an overall data on the affinity obtained from the mean of the dissociation constants of all the species present in solution regardless of their stoichiometries and structures, at a specific pH value [43,66].

At pH 7.4, the K_D^{app} for copper complexes formed by dNGF(1-15) and NGF(1-14) are higher than those calculated for complexes of rNGF(14-1) and sNGF(1-14), confirming that the presence of a His closest to N-terminal group allows the formation of a more stable copper complex (Table 4).

Table 4. Apparent dissociation constant values for copper(II) complexes.

Peptide	pH	K_D^{app}
NGF(1-14)	7.4	2.5×10^{-11}
dNGF(1-15)	7.4	4.2×10^{-11}
rNGF(14-1)	7.4	6.5×10^{-10}
sNGF(1-14)	7.4	2.7×10^{-10}
$A\beta_{1\text{-}16}$-PEG [a]	7.4	1.1×10^{-10}
$hCtr_{1\text{-}14}$ [b]	7.4	1.0×10^{-13}
NGF(1-14)	5.5	4.0×10^{-6}
dNGF(1-15)	5.5	1.9×10^{-7}
rNGF(14-1)	5.5	1.4×10^{-5}
sNGF(1-14)	5.5	3.8×10^{-5}
$A\beta_{1\text{-}16}$-PEG	5.5	2.5×10^{-7}
$hCtr_{1\text{-}14}$	5.5	7.4×10^{-8}

[a] Reference [54]; [b] Reference [40].

The affinity values for copper ions of a peptide encompassing the sequence 1-16 of Aβ, functionalized with a polyethylene glycol moiety ($A\beta_{1\text{-}16}$-PEG) to increase peptide solubility, were calculated from reported stability constant values [54]. Analogously, the K_D^{app} values for copper complexes formed by the N-terminal fragment of hCtr-1 were calculated from potentiometric data reported in literature [40].

The comparison with the K_D^{app} of copper complex formed by Aβ1-16, shows that both NGF(1-14) and dNGF(1-15) bind a single copper ion with higher affinity than Aβ fragment but lesser than $hCtr_{1\text{-}14}$.

It has been hypothesized that Aβ can chelate copper ions in the synaptic cleft and act as an extracellular metal chaperone for its delivery to hCtr1 protein. The release of copper from Aβ should be driven by the higher affinity of hCtr1 [40,41]. In competition with Aβ, NGF could perform a similar activity transporting copper to hCtr1. On the other hand, NGF having a high affinity for copper binding may capture copper ions in the synaptic cleft for different aims as cellular metal uptake through different pathways or neurons protection from metal excess. It is worth noting that copper addition increases activity of NGF as well as those of its N-terminal mimicking peptides. The pivotal role of copper is evidenced also by a general inhibitory effect on NGF and related peptides signaling cascade, determined by the addition of the bathocuproine disulfonic acid, a copper chelating agent [14,21].

Differently, at acidic pH the $A\beta_{1\text{-}16}$-PEG peptide shows a higher affinity compared to the investigated NGF peptides even though the difference with dNGF(1-15) constant value is minimal. The peptide hCtr1-14 displays higher affinity for copper ions also at pH 5.5, so Aβ may act as metal chaperon for copper uptake in this environmental condition. However, it worth noting that a slight acidic pH promotes Aβ fibrils aggregation, limiting the chelation of copper by polypeptide. The combinations of these factors may determine toxicity and insult to neurons [67,68].

4. Conclusions

Potentiometric experiments carried out on N-terminal NGF peptides show that they bind metal with high affinity. NGF peptides are able to bind only one copper ion, even though they have more copper anchoring sites, differently from Aβ polypeptide that form multinuclear complex species. Therefore, the molar peptide-to-metal molar ratio can determine a different speciation between components present simultaneously at the synapses.

The determination of affinity constant values for copper ion indicates that at physiological pH and equimolar concentration, NGF peptides can compete with Aβ fragment for copper binding. Therefore, NGF could play a role in controlling copper homeostasis in the synaptic space as suggested for Aβ. This finding may partially explain the activity of copper complexes formed by N-terminal NGF peptides, which are able to promote CREB phosphorylation, a process pivotal to memory formation [14].

A slightly more acidic pH would make Aβ polypeptide, the most suitable ligand for copper release to hCtr1 compared with NGF peptides. In this environmental condition, NGF activity related also to the presence of copper ions could be limited with potential consequences on neuron physiology.

5. Materials and Methods

5.1. Chemicals

The peptides VFSEGRHFIPHSSS-NH2, rNGF(14-1) and GFRESPHVSISSH-NH2 sNGF (1-14) the scrambled sNGF(1-14) were synthesized) with the amidated C-terminal and purified as previously reported [14]. The dimer dNGF(1-15) was purchased from CASLO (Kongens Lyngby, Denmark).

All other chemicals, of the highest available grade, were purchased from Sigma-Aldrich (Munich, Germany) and used without further purification.

5.2. Potentiometric Titrations

Potentiometric titrations were performed on automatic instrument Titrando 905. A combined glass-Ag/AgCl electrode (Metrohm, Herisau, Switzerland) was used. All measurements were carried out on 2.0 mL of samples aqueous solutions of samples kept under an argon atmosphere and at a temperature of 298 K by means of a thermostat. Other details on the electrode calibration have been previously reported [69]. The ionic strength was fixed at 0.1 M by adding KNO_3. KOH 0.1 M was used to titrate solutions containing either the free peptide or the peptide with Cu^{2+}. The peptide concentrations used were 1×10^{-3} M. At least four independent titrations were performed. At the beginning of each measurement, the pH value was adjusted to 2.4 by addition of HNO_3 0.2 M and measurements were carried out up to pH 11. Metal ion to ligand molar ratios between 0.9:1 and 2.2:1 were used. The experimental data were analyzed by using HYPERQUAD 2003 program [70] and species distribution as a function of pH was obtained by means of Hyss program [71].

5.3. UV–Vis and CD Measurements

UV–vis spectra were recorded at 298.0 ± 0.2 K, by using an Agilent 8453 spectrophotometer. All the solutions were freshly prepared using double distilled water. UV–vis spectra were acquired by using 1.0×10^{-3} M peptide concentration at 1:1 metal to ligand molar ratio. The results are reported as ε (molar adsorption coefficient).

CD spectra were obtained at 25 °C under a constant N_2 flow on a Jasco model 810 spectropolarimeter at a scan rate of 25 nm min^{-1}, resolution of 0.1 nm, path length 1cm. Calibration of the instrument was performed with a 0.06% aqueous solution of ammonium camphorsulfonate. Spectra were recorded as an average of five scans. The CD spectra of the copper(II) complexes on varying the solution pH were obtained in the 280–750 nm wavelength region. CD spectra were acquired by using 1×10^{-3} peptide concentration at 1:1 metal to ligand molar ratio. The results are reported as Δε (molar circular dichroism), calculated as $\Delta\varepsilon = [\theta]/3298.2$ [72].

Author Contributions: D.L.M., A.M., and E.R. conceived and designed the experiments; A.M. and D.L.M. performed the experiments; D.L.M., A.M., and E.R. wrote the paper. All authors have read and agreed to the published version of the manuscript.

Funding: Beneficentia Stiftung, Vaduz (grant N. BEN2019/48).

Institutional Review Board Statement: Not applicable.

Informed Consent Statement: Not applicable.

Data Availability Statement: All data are available from the corresponding author on request.

Acknowledgments: Authors thank the University Consortium for Research in the Chemistry of Metal ions in Biological Systems (CIRCMSB); D.L. thanks Beneficentia Stiftung, Vaduz (BEN2019/48).

Conflicts of Interest: The authors declare no conflict of interest. The founding sponsors had no role in the design of the study; in the collection, analyses, or interpretation of data; in the writing of the manuscript, or in the decision to publish the results.

References

1. Scheiber, I.F.; Mercer, J.F.; Dringen, R. Metabolism and functions of copper in brain. *Prog. Neurobiol.* **2014**, *116*, 33–57. [CrossRef]
2. Ackerman, C.M.; Chang, C.J. Copper signaling in the brain and beyond. *J. Biol. Chem.* **2018**, *293*, 4628–4635. [CrossRef]
3. Lutsenko, S.; Washington-Hughes, C.; Ralle, M.; Schmidt, K. Copper and the brain noradrenergic system. *J. Biol. Inorg. Chem.* **2019**, *24*, 1179–1188. [CrossRef] [PubMed]
4. Grubman, A.; White, A.R. Copper as a key regulator of cell signalling pathways. *Expert Rev. Mol. Med.* **2014**, *16*, e11. [CrossRef] [PubMed]
5. Kardos, J.; Héja, L.; Simon, Á.; Jablonkai, I.; Kovács, R.; Jemnitz, K. Copper signalling: Causes and consequences. *Cell Commun. Signal.* **2018**, *16*. [CrossRef] [PubMed]
6. La Mendola, D.; Giacomelli, C.; Rizzarelli, E. Intracellular Bioinorganic Chemistry and Cross Talk Among Different -Omics. *Curr. Top. Med. Chem.* **2016**, *16*, 3103–3130. [CrossRef] [PubMed]
7. Kardos, J.; Kovács, I.; Hajós, F.; Kálmán, M.; Simonyi, M. Nerve endings from rat brain tissue release copper upon depolarization. A possible role in regulating neuronal excitability. *Neurosci. Lett.* **1989**, *103*, 139–144. [CrossRef]
8. D'Ambrosi, N.; Rossi, L. Copper at synapse: Release, binding and modulation of neurotransmission. *Neurochem. Int.* **2015**, *90*, 36–45. [CrossRef] [PubMed]
9. Kapkaeva, M.R.; Popova, O.V.; Kondratenko, R.V.; Rogozin, P.D.; Genrikhs, E.E.; Stelmashook, E.V.; Skrebitsky, V.G.; Khaspekov, L.G.; Isaev, N.K. Effects of copper on viability and functional properties of hippocampal neurons in vitro. *Exp. Toxicol. Pathol.* **2017**, *69*, 259–264. [CrossRef]
10. Nam, E.; Nam, G.; Lim, M.H. Synaptic Copper, Amyloid-β, and Neurotransmitters in Alzheimer's Disease. *Biochemistry* **2020**, *59*, 15–17. [CrossRef]
11. Garcia-Osta, A.; Alberini, C.M. Amyloid beta mediates memory formation. *Learn. Mem.* **2009**, *16*, 267–272. [CrossRef] [PubMed]
12. Parihar, M.S.; Brewer, G.J. Amyloid-β as a modulator of synaptic plasticity. *J. Alzheimers Dis.* **2010**, *22*, 741–763. [CrossRef]
13. Zimbone, S.; Monaco, I.; Gianì, F.; Pandini, G.; Copani, A.G.; Giuffrida, M.L.; Rizzarelli, E. Amyloid Beta monomers regulate cyclic adenosine monophosphate response element binding protein functions by activating type-1 insulin-like growth factor receptors in neuronal cells. *Aging Cell* **2018**, *17*, e12684. [CrossRef]
14. Naletova, I.; Satriano, C.; Pietropaolo, A.; Gianì, F.; Pandini, G.; Triaca, V.; Amadoro, G.; Latina, V.; Calissano, P.; Travaglia, A.; et al. The Copper(II)-Assisted Connection between NGF and BDNF by Means of Nerve Growth Factor-Mimicking Short Peptides. *Cells* **2019**, *8*, 301. [CrossRef]
15. Levi-Montalcini, R. The nerve growth factor 35 years later. *Science* **1987**, *237*, 1154–1162. [CrossRef] [PubMed]
16. Sofroniew, M.V.; Howe, C.L.; Mobley, W.C. Nerve growth factor signaling, neuroprotection, and neural repair. *Annu. Rev. Neurosci.* **2001**, *24*, 1217–1281. [CrossRef] [PubMed]
17. Conner, J.M.; Franks, K.M.; Titterness, A.K.; Russell, K.; Merrill, D.A.; Christie, B.R.; Sejnowski, T.J.; Tuszynski, M.H. NGF is essential for hippocampal plasticity and learning. *J. Neurosci.* **2009**, *29*, 10883–10889. [CrossRef]
18. Reichardt, L.F. Neurotrophin-regulated signalling pathways. *Philos. Trans. R. Soc. Lond. B Biol. Sci.* **2006**, *361*, 1545–1564. [CrossRef]
19. Riccio, A.; Pierchala, B.A.; Ciarallo, C.L.; Ginty, D.D. An NGF-TrkA-mediated retrograde signal to transcription factor CREB in sympathetic neurons. *Science* **1997**, *277*, 1097–1100. [CrossRef]
20. Travaglia, A.; Arena, G.; Fattorusso, R.; Isernia, C.; La Mendola, D.; Malgieri, G.; Nicoletti, V.G.; Rizzarelli, E. The inorganic perspective of nerve growth factor: Interactions of Cu^{2+} and Zn^{2+} with the N-terminus fragment of nerve growth factor encompassing the recognition domain of the TrkA receptor. *Chemistry* **2011**, *17*, 3726–3738. [CrossRef]
21. Pandini, G.; Satriano, C.; Pietropaolo, A.; Gianì, F.; Travaglia, A.; La Mendola, D.; Nicoletti, V.G.; Rizzarelli, E. The Inorganic Side of NGF: Copper(II) and Zinc(II) Affect the NGF Mimicking Signaling of the N-Terminus Peptides Encompassing the Recognition Domain of TrkA Receptor. *Front. Neurosci.* **2016**, *10*. [CrossRef]

22. Mufson, E.J.; Counts, S.E.; Ginsberg, S.D.; Mahady, L.; Perez, S.E.; Massa, S.M.; Longo, F.M.; Ikonomovic, M.D. Nerve Growth Factor Pathobiology during the Progression of Alzheimer's Disease. *Front. Neurosci.* **2019**, *13*. [CrossRef] [PubMed]
23. Matrone, C.; Ciotti, M.T.; Mercanti, D.; Marolda, R.; Calissano, P. NGF and BDNF signaling control amyloidogenic route and Abeta production in hippocampal neurons. *Proc. Natl. Acad. Sci. USA* **2008**, *105*, 13139–13144. [CrossRef]
24. Canu, N.; Pagano, I.; La Rosa, L.R.; Pellegrino, M.; Ciotti, M.T.; Mercanti, D.; Moretti, F.; Sposato, V.; Triaca, V.; Petrella, C.; et al. Association of TrkA and APP Is Promoted by NGF and Reduced by Cell Death-Promoting Agents. *Front. Mol. Neurosci.* **2017**, *10*. [CrossRef]
25. Canu, N.; Amadoro, G.; Triaca, V.; Latina, V.; Sposato, V.; Corsetti, V.; Severini, C.; Ciotti, M.T.; Calissano, P. The Intersection of NGF/TrkA Signaling and Amyloid Precursor Protein Processing in Alzheimer's Disease Neuropathology. *Int. J. Mol. Sci.* **2017**, *18*, 1319. [CrossRef] [PubMed]
26. Su, R.; Su, W.; Jiao, Q. NGF protects neuroblastoma cells against β-amyloid-induced apoptosis via the Nrf2/HO-1 pathway. *FEBS Open Bio* **2019**, *9*, 2063–2071. [CrossRef]
27. Sáez, E.T.; Pehar, M.; Vargas, M.R.; Barbeito, L.; Maccioni, R.B. Production of nerve growth factor by beta-amyloid-stimulated astrocytes induces p75NTR-dependent tau hyperphosphorylation in cultured hippocampal neurons. *J. Neurosci. Res.* **2006**, *84*, 1098–1106. [CrossRef] [PubMed]
28. Ejaz, H.W.; Wang, W.; Lang, M. Copper Toxicity Links to Pathogenesis of Alzheimer's Disease and Therapeutics Approaches. *Int. J. Mol. Sci.* **2020**, *21*, 7660. [CrossRef]
29. Kaden, D.; Bush, A.I.; Danzeisen, R.; Bayer, T.A.; Multhaup, G. Disturbed copper bioavailability in Alzheimer's disease. *Int. J. Alzheimers Dis.* **2011**, *2011*. [CrossRef]
30. Barnham, K.J.; Bush, A.I. Metals in Alzheimer's and Parkinson's diseases. *Curr. Opin. Chem. Biol.* **2008**, *12*, 222–228. [CrossRef]
31. Lovell, M.A.; Robertson, J.D.; Teesdale, W.J.; Campbell, J.L.; Markesbery, W.R. Copper, iron and zinc in Alzheimer's disease senile plaques. *J. Neurol. Sci.* **1998**, *158*, 47–52. [CrossRef]
32. Bagheri, S.; Squitti, R.; Haertlé, T.; Siotto, M.; Saboury, A.A. Role of Copper in the Onset of Alzheimer's Disease Compared to Other Metals. *Front. Aging Neurosci.* **2018**, *9*. [CrossRef]
33. Exley, C.; House, E.; Polwart, A.; Esiri, M.M. Brain burdens of aluminum, iron, and copper and their relationships with amyloid-β pathology in 60 human brains. *J. Alzheimers Dis.* **2012**, *31*, 725–730. [CrossRef]
34. Scholefield, M.; Church, S.J.; Xu, J.; Patassini, S.; Roncaroli, F.; Hooper, N.M.; Unwin, R.D.; Cooper, G.J.S. Widespread Decreases in Cerebral Copper Are Common to Parkinson's Disease Dementia and Alzheimer's Disease Dementia. *Front. Aging Neurosci.* **2021**, *13*. [CrossRef] [PubMed]
35. Squitti, R.; Siotto, M.; Polimanti, R. Low-copper diet as a preventive strategy for Alzheimer's disease. *Neurobiol. Aging* **2014**, *35* (Suppl. 2), S40–S50. [CrossRef]
36. Behzadfar, L.; Abdollahi, M.; Sabzevari, O.; Hosseini, R.; Salimi, A.; Naserzadeh, P.; Sharifzadeh, M.; Pourahmad, J. Potentiating role of copper on spatial memory deficit induced by beta amyloid and evaluation of mitochondrial function markers in the hippocampus of rats. *Metallomics* **2017**, *9*, 969–980. [CrossRef] [PubMed]
37. Squitti, R.; Ventriglia, M.; Gennarelli, M.; Colabufo, N.A.; El Idrissi, I.G.; Bucossi, S.; Mariani, S.; Rongioletti, M.; Zanetti, O.; Congiu, C.; et al. Non-Ceruloplasmin Copper Distincts Subtypes in Alzheimer's Disease: A Genetic Study of ATP7B Frequency. *Mol. Neurobiol.* **2017**, *54*, 671–681. [CrossRef]
38. Zhao, J.; Shi, Q.; Tian, H.; Li, Y.; Liu, Y.; Xu, Z.; Robert, A.; Liu, Q.; Meunier, B. TDMQ20, a Specific Copper Chelator, Reduces Memory Impairments in Alzheimer's Disease Mouse Models. *ACS Chem. Neurosci.* **2021**, *12*, 140–149. [CrossRef] [PubMed]
39. Wang, L.; Yin, Y.L.; Liu, X.Z.; Shen, P.; Zheng, Y.G.; Lan, X.R.; Lu, C.B.; Wang, J.Z. Current understanding of metal ions in the pathogenesis of Alzheimer's disease. *Transl. Neurodegener.* **2020**, *9*. [CrossRef]
40. Stefaniak, E.; Pushie, M.J.; Vaerewyck, C.; Corcelli, D.; Griggs, C.; Lewis, W.; Kelley, E.; Maloney, N.; Sendzik, M.; Bal, W.; et al. Exploration of the Potential Role for Aβ in Delivery of Extracellular Copper to Ctr1. *Inorg. Chem.* **2020**, *59*, 16952–16966. [CrossRef]
41. Stefaniak, E.; Bal, W. Cu^{II} Binding Properties of N-Truncated Aβ Peptides: In Search of Biological Function. *Inorg. Chem.* **2019**, *58*, 13561–13577. [CrossRef] [PubMed]
42. Alies, B.; Bijani, C.; Sayen, S.; Guillon, E.; Faller, P.; Hureau, C. Copper coordination to native N-terminally modified versus full-length amyloid-β: Second-sphere effects determine the species present at physiological pH. *Inorg. Chem.* **2012**, *51*, 12988–13000. [CrossRef] [PubMed]
43. Arena, G.; Pappalardo, G.; Sovago, I.; Rizzarelli, E. Copper(II) interaction with amyloid-β: Affinity and speciation. *Coord. Chem. Rev.* **2012**, *256*, 3–12. [CrossRef]
44. Lyros, E.; Ragoschke-Schumm, A.; Kostopoulos, P.; Sehr, A.; Backens, M.; Kalampokini, S.; Decker, Y.; Lesmeister, M.; Liu, Y.; Reith, W.; et al. Normal brain aging and Alzheimer's disease are associated with lower cerebral pH: An in vivo histidine ^{1}H-MR spectroscopy study. *Neurobiol. Aging* **2020**, *87*, 60–69. [CrossRef] [PubMed]
45. Decker, Y.; Németh, E.; Schomburg, R.; Chemla, A.; Fülöp, L.; Menger, M.D.; Liu, Y.; Fassbender, K. Decreased pH in the aging brain and Alzheimer's disease. *Neurobiol. Aging* **2021**, *101*, 40–49. [CrossRef]
46. Tóth, M.O.; Menyhárt, Á.; Frank, R.; Hantosi, D.; Farkas, E.; Bari, F. Tissue Acidosis Associated with Ischemic Stroke to Guide Neuroprotective Drug Delivery. *Biology* **2020**, *9*, 460. [CrossRef] [PubMed]

47. Su, Y.; Chang, P.T. Acidic pH promotes the formation of toxic fibrils from beta-amyloid peptide. *Brain Res.* **2001**, *893*, 287–291. [CrossRef]
48. Grasso, G.; Magrì, A.; Bellia, F.; Pietropaolo, A.; La Mendola, D.; Rizzarelli, E. The copper(II) and zinc(II) coordination mode of HExxH and HxxEH motif in small peptides: The role of carboxylate location and hydrogen bonding network. *J. Inorg. Biochem.* **2014**, *130*, 92–102. [CrossRef]
49. Rajković, S.; Kállay, C.; Serényi, R.; Malandrinos, G.; Hadjiliadis, N.; Sanna, D.; Sóvágó, I. Complex formation processes of terminally protected peptides containing two or three histidyl residues. Characterization of the mixed metal complexes of peptides. *Dalton Trans.* **2008**, *37*, 5059–5071. [CrossRef]
50. Kállay, C.; Várnagy, K.; Micera, G.; Sanna, D.; Sóvágó, I. Copper(II) complexes of oligopeptides containing aspartyl and glutamyl residues. Potentiometric and spectroscopic studies. *J. Inorg. Biochem.* **2005**, *99*, 1514–1525. [CrossRef]
51. La Mendola, D.; Magrì, A.; Campagna, T.; Campitiello, M.A.; Raiola, L.; Isernia, C.; Hansson, O.; Bonomo, R.P.; Rizzarelli, E. A doppel alpha-helix peptide fragment mimics the copper(II) interactions with the whole protein. *Chemistry* **2010**, *16*, 6212–6223. [CrossRef]
52. Karavelas, T.; Malandrinos, G.; Hadjiliadis, N.; Mlynarz, P.; Kozlowski, H.; Barsan, M.; Butler, I. Coordination properties of Cu(II) and Ni(II) ions towards the C-terminal peptide fragment -TYTEHA- of histone H4. *Dalton Trans.* **2008**, *9*, 1215–1223. [CrossRef]
53. Kowalik-Jankowska, T.; Ruta, M.; Wiśniewska, K.; Lankiewicz, L. Coordination abilities of the 1-16 and 1-28 fragments of beta-amyloid peptide towards copper(II) ions: A combined potentiometric and spectroscopic study. *J. Inorg. Biochem.* **2003**, *95*, 270–282. [CrossRef]
54. Damante, C.A.; Osz, K.; Nagy, Z.; Pappalardo, G.; Grasso, G.; Impellizzeri, G.; Rizzarelli, E.; Sóvágó, I. The metal loading ability of beta-amyloid N-terminus: A combined potentiometric and spectroscopic study of copper(II) complexes with beta-amyloid(1-16), its short or mutated peptide fragments, and its polyethylene glycol (PEG)-ylated analogue. *Inorg. Chem.* **2008**, *47*, 9669–9683. [CrossRef] [PubMed]
55. Magrì, A.; Munzone, A.; Peana, M.; Medici, S.; Zoroddu, M.A.; Hansson, O.; Satriano, C.; Rizzarelli, E.; La Mendola, D. Coordination Environment of Cu(II) Ions Bound to N-Terminal Peptide Fragments of Angiogenin Protein. *Int. J. Mol. Sci.* **2016**, *17*, 1240. [CrossRef]
56. Kállay, C.; Nagy, Z.; Várnagy, K.; Malandrinos, G.; Hadjiliadis, N.; Sóvágó, I. Thermodynamic and structural characterization of the copper(II) complexes of peptides containing both histidyl and aspartyl residues. *Bioinorg. Chem. Appl.* **2007**, *2007*. [CrossRef]
57. La Mendola, D.; Magrì, A.; Hansson, Ö.; Bonomo, R.P.; Rizzarelli, E. Copper(II) complexes with peptide fragments encompassing the sequence 122-130 of human doppel protein. *J. Inorg. Biochem.* **2009**, *103*, 758–765. [CrossRef] [PubMed]
58. Matera, A.; Brasuń, J.; Cebrat, M.; Świątek-Kozłowska, J. The role of the histidine residue in the coordination abilities of peptides with a multi-histidine sequence towards copper(II) ions. *Polyhedron* **2008**, *27*, 1539–1555. [CrossRef]
59. Zoroddu, M.A.; Kowalik-Jankowska, T.; Medici, S.; Peana, M.; Kozlowski, H. Copper(II) binding to Cap43 protein fragments. *Dalton Trans.* **2008**, *44*, 6127–6134. [CrossRef]
60. Pontecchiani, F.; Simonovsky, E.; Wieczorek, R.; Barbosa, N.; Rowinska-Zyrek, M.; Potocki, S.; Remelli, M.; Miller, Y.; Kozlowski, H. The unusual binding mechanism of Cu(II) ions to the poly-histidyl domain of a peptide found in the venom of an African viper. *Dalton Trans.* **2014**, *43*, 16680–16689. [CrossRef] [PubMed]
61. Pietropaolo, A.; Muccioli, L.; Zannoni, C.; La Mendola, D.; Maccarrone, G.; Pappalardo, G.; Rizzarelli, E. Unveiling the role of histidine and tyrosine residues on the conformation of the avian prion hexarepeat domain. *J. Phys. Chem. B* **2008**, *112*, 5182–5188. [CrossRef]
62. Bataille, M.; Formicka-Kozlowska, G.; Kozlowski, H.; Pettit, L.D.; Steel, I. The L-proline residue as a 'break-point' in the co-ordination of metal–peptide systems. *J. Chem. Soc. Chem. Commun.* **1984**, 231–232. [CrossRef]
63. Magrì, A.; Tabbì, G.; Breglia, R.; De Gioia, L.; Fantucci, P.; Bruschi, M.; Bonomo, R.P.; La Mendola, D. Copper ion interaction with the RNase catalytic site fragment of the angiogenin protein: An experimental and theoretical investigation. *Dalton Trans.* **2017**, *46*, 8524–8538. [CrossRef]
64. La Mendola, D.; Arena, G.; Pietropaolo, A.; Satriano, C.; Rizzarelli, E. Metal ion coordination in peptide fragments of neurotrophins: A crucial step for understanding the role and signaling of these proteins in the brain. *Coord. Chem. Rev.* **2021**, *435*. [CrossRef]
65. Murphy, J.M.; Powell, B.A.; Brumaghim, J.L. Stability constants of bio-relevant, redox-active metals with amino acids: The challenges of weakly binding ligands. *Coord. Chem. Rev.* **2020**, *412*. [CrossRef]
66. Tõugu, V.; Karafin, A.; Palumaa, P. Binding of zinc(II) and copper(II) to the full-length Alzheimer's amyloid-beta peptide. *J. Neurochem.* **2008**, *104*, 1249–1259. [CrossRef] [PubMed]
67. Paredes-Rosan, C.A.; Valencia, D.E.; Barazorda-Ccahuana, H.L.; Aguilar-Pineda, J.A.; Gómez, B. Amyloid beta oligomers: How pH influences over trimer and pentamer structures? *J. Mol. Model.* **2020**, *26*, 1–8. [CrossRef]
68. Liao, Q.; Owen, M.C.; Bali, S.; Barz, B.; Strodel, B. Aβ under stress: The effects of acidosis, Cu^{2+}-binding, and oxidation on amyloid β-peptide dimers. *Chem. Commun.* **2018**, *54*, 7766–7769. [CrossRef]
69. Amorini, A.M.; Bellia, F.; Di Pietro, V.; Giardina, B.; La Mendola, D.; Lazzarino, G.; Sortino, S.; Tavazzi, B.; Rizzarelli, E.; Vecchio, G. Synthesis and antioxidant activity of new homocarnosine beta-cyclodextrin conjugates. *Eur. J. Med. Chem.* **2007**, *42*, 910–920. [CrossRef]

70. Gans, P.; Sabatini, A.; Vacca, A. Investigation of equilibria in solution. Determination of equilibrium constants with the HYPERQUAD suite of programs. *Talanta* **1996**, *43*, 1739–1753. [CrossRef]
71. Alderighi, L.; Gans, P.; Ienco, A.; Peters, D.; Sabatini, A.; Vacca, A. Hyperquad simulation and speciation (HySS): A utility program for the investigation of equilibria involving soluble and partially soluble species. *Coord. Chem. Rev.* **1999**, *184*, 311–318. [CrossRef]
72. Bellia, F.; La Mendola, D.; Maccarrone, G.; Mineo, P.; Vitalini, D.; Scamporrino, E.; Sortino, S.; Vecchio, G.; Rizzarelli, E. Copper(II) complexes with β-cyclodextrin–homocarnosine conjugates and their antioxidant activity. *Inorg. Chim. Acta* **2007**, *360*, 945–954. [CrossRef]